

Article

Dynamic Modeling and Simulation on a Hybrid Power System for Electric Vehicle Applications

Hong-Wen He ^{1,*}, Rui Xiong ¹ and Yu-Hua Chang ²

¹ National Engineering Laboratory for Electric Vehicles, Beijing Institute of Technology, Beijing, 10081, China; E-Mail: bityan@bit.edu.cn (R.X.)

² The Faculty of Automotive and Construction Machinery Engineering, Warsaw University of Technology, Warsaw, 02-524, Poland; E-Mail: yuhua.chang@simr.pw.edu.pl

* Author to whom correspondence should be addressed; E-Mail: hwhebit@bit.edu.cn; Tel.: +86-10-6891-4842; Fax: +86-10-6891-4842.

Received: 30 August 2010; in revised form: 7 October 2010 / Accepted: 16 November 2010 /

Published: 22 November 2010

Abstract: Hybrid power systems, formed by combining high-energy-density batteries and high-power-density ultracapacitors in appropriate ways, provide high-performance and high-efficiency power systems for electric vehicle applications. This paper first establishes dynamic models for the ultracapacitor, the battery and a passive hybrid power system, and then based on the dynamic models a comparative simulation between a battery only power system and the proposed hybrid power system was done under the UDDS (Urban Dynamometer Driving Schedule). The simulation results showed that the hybrid power system could greatly optimize and improve the efficiency of the batteries and their dynamic current was also decreased due to the participation of the ultracapacitors, which would have a good influence on batteries' cycle life. Finally, the parameter matching for the passive hybrid power system was studied by simulation and comparisons.

Keywords: ultracapacitor; battery; hybrid power system; dynamic modeling; electric vehicles

1. Introduction

With the appearance of 89 kinds of new-energy vehicles in the 2010 Beijing Auto Show, various types of Electric Vehicles (EVs), like pure electric vehicles, hybrid electric vehicles and fuel cell electric vehicles, have begun to appear on the market [1,2]. Batteries are usually selected as the electric

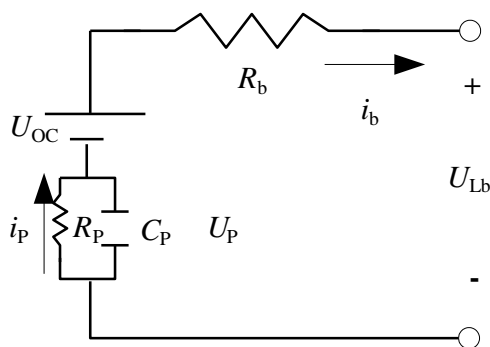
energy storage system of EVs [3], but when a longer purely electric driving range (*i.e.*, higher energy), higher acceleration rates, and higher power-assisted performance (*i.e.*, higher power) are required simultaneously, as in plug-in hybrid electric vehicles, it is hard for a battery-only power system to meet these demands. One solution is to select more costly larger capacity batteries, which would increase the vehicle weight and decrease the vehicle economy. Another solution is to maintain the original battery capacity and to overcharge or overdischarge the battery, which would decrease its lifespan and make it work at lower efficiency. This dilemma suggests combining together batteries and ultracapacitors to form hybrid power systems as a promising solution to these problems because the ultracapacitor has a higher specific power and much longer lifespan than a battery, despite the fact that its energy density is much smaller than that of a battery [4]. The hybrid power system then benefits from the mutual compromise by integrating the advantages and avoiding the disadvantages of batteries and ultracapacitors. Topology and control strategy are key technologies of the hybrid power system, which have a great influence on the energy density, power density, efficiency and ultimate cost of hybrid power systems [5–8]. In comparison, the passive topology, which directly combines ultracapacitors and batteries in parallel, is the simplest one with the least complicated control strategy. This paper mainly discusses the passive hybrid power system to check its advantages and find a reasonable way to match its parameters.

2. Dynamic Modeling for Hybrid Power System

2.1. Dynamic Model of the Battery

Compared with other battery models, the Thevenin model is more suitable for modeling lithium-ion batteries [9]. Its topology is shown in Figure 1, where U_{OC} represents an ideal voltage source, which describes the battery open-circuit voltage; R_b is ohm resistance; Polarization resistance R_p and polarization capacitance C_p describe the battery's over-voltage U_p , used to describe the dynamic characteristics of the battery; i_b and U_{Lb} are the load current and load voltage of the battery, respectively.

Figure 1. Thevenin battery model.



In order to indicate the residual electricity of the battery, State of Charge (*SoC*) is traditional used, which is defined by Equation (1):

$$SoC = SoC_0 - k_{ch} \times k_{dis} \times \frac{\int \eta \times i_b dt}{C_N} \tag{1}$$

where SoC_0 is the initial value of SoC ; C_N is the nominal capacity of battery; η is the coulomb efficiency (including discharging efficiency η_{dis} and charging efficiency η_{ch}); k_{ch} and k_{dis} are the influence coefficients on the current integration from charging current ($i_b < 0$) and discharging current ($i_b \geq 0$) respectively, if the battery is charging, $k_{dis} = 1$, if the battery is discharging, $k_{ch} = 1$.

The main state equation for the Thevenin battery model is given by Equation (2):

$$\begin{cases} \dot{U}_P = -\frac{U_P}{C_P R_P} + \frac{i_b}{C_P} \\ U_{Lb} = -U_P + U_{OC} - i_b R_b \end{cases} \tag{2}$$

The Hybrid Pulse Power Characterization (HPPC) test [10] was implemented for a lithium-ion battery module with a nominal voltage of 57.6 V and a nominal capacity of 30 Ah. The model parameter results identified using the robust least squares method are listed in Table 1 [11].

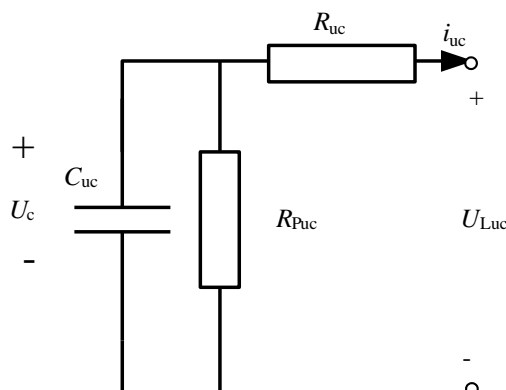
Table 1. The list of the identification results of lithium-ion battery model parameters.

$SoC/\%$	U_{OC}/V	C_p/F	$R_p/(m\Omega)$	$R_b/(m\Omega)$
100	66.504	657.89	6.84	24.08
90	65.252	429.58	7.15	23.95
80	64.810	502.51	7.96	24.03
70	64.247	666.67	7.50	24.06
60	63.799	691.56	7.23	24.21
50	63.302	683.23	8.05	24.26
40	62.679	511.36	8.88	24.53
30	61.832	725.51	8.27	24.54
20	61.160	862.07	9.28	24.66
10	60.125	760.65	9.86	24.80

2.2. Dynamic Model of the Ultracapacitor

To model the ultracapacitor, a circuit model topology is selected, as shown in Figure 2 [12].

Figure 2. The circuit topology of ultracapacitor model.



Here R_{uc} is ohm resistance; R_{Puc} is self-discharge resistance, which is much larger than R_{uc} ; i_{uc} , U_{Luc} , U_c are load current, load voltage and terminal voltage of the ultracapacitor, respectively. Although the manufacturer provides a nominal capacity for the ultracapacitor, the actual capacity must still be verified experimentally, and the main calculated expression is as given by Equation (3):

$$C_{uc} = \frac{\int i_{uc} dt}{\Delta U_{Luc}} \tag{3}$$

where ΔU_{Luc} is the variation of load voltage during the constant-current experiment.

The load voltage can be calculated using Equation (4):

$$\begin{cases} \dot{U}_c = \frac{-U_c}{C_{uc} R_{Puc}} + \frac{i_{uc}}{C_{uc}} \\ U_{Luc} = U_c - R_{uc} i_{uc} \end{cases} \tag{4}$$

In order to indicate the residual electricity of ultracapacitor, State of Voltage (SoV) [13] is used and defined as in Equation (5):

$$SoV = \frac{U_{Luc}}{U_{cmax}} \tag{5}$$

where U_{cmax} is the nominal voltage of the ultracapacitor.

Based on the experiment data of an ultracapacitor module with nominal voltage of 16.8 V and nominal capacity of 500 F, using the robust least squares method, the model parameters R_{uc} , C_{uc} , which are the function of i_{uc} , and R_{Puc} are identified as in Tables 2–4, respectively.

Table 2. The list of the identification results of R_{uc} .

i_{uc}/A	-2.22	-20	-50	-100	-150	-200
$R_{uc}/(m\Omega)$	2.41	2.14	1.96	1.94	1.84	1.83
i_{uc}/A	2.22	20	50	100	150	200
$R_{uc}/(m\Omega)$	2.36	2.01	1.96	1.8	1.76	1.75

Table 3. The list of the identification results of C_{uc} .

i_{uc}/A	20	50	100	150	200
C_{uc}/F	471.1	468.9	469	467.3	465.2
i_{uc}/A	-20	-50	-100	-150	-200
C_{uc}/F	486.7	487.7	487.1	488.4	486.6

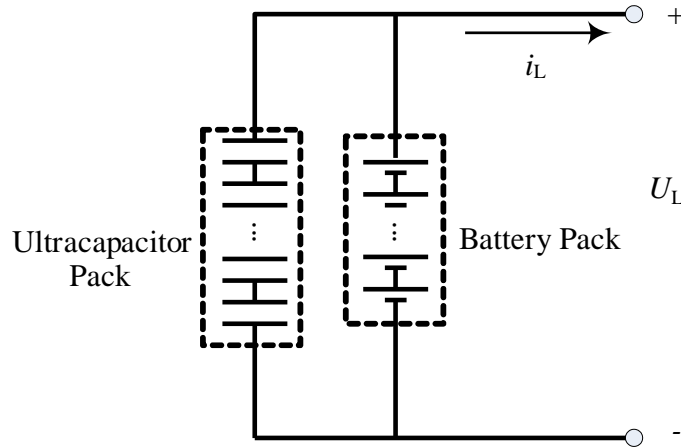
Table 4. The list of the identification results of R_{Puc} .

	Discharging	Charging
R_{Puc}/Ω	12.43	1.11

2.3. Dynamic Model of the Hybrid Power System

A passive hybrid power system with the topology as shown in Figure 3 is selected. For use in EVs, the output power from battery pack and ultracapacitor pack must meet the motor’s driving power requirements.

Figure 3. The circuit topology of a passive hybrid power system.



Since the battery pack and ultracapacitor pack are directly connected in parallel, given a certain power load profile P_m , the battery current i_b and ultracapacitor current i_{uc} can be found from basic circuit rules like Kirchhoff’s voltage and current laws:

$$i_L = i_b + i_{uc} \tag{6}$$

$$\begin{cases} U_L = U_c - i_{uc}R_{uc} \\ U_L = U_{OC} - i_bR_b - U_P \end{cases} \tag{7}$$

$$i_{uc} = C_{uc} \frac{dU_c}{dt} \tag{8}$$

$$\frac{dU_c}{dt} = \frac{U_c + i_L R_b - (U_{OC} - U_P)}{\tau_{hps}} \Rightarrow U_c = U_{OC} - i_L R_b - U_P + \exp\left(\frac{t}{\tau_{hps}}\right) \times \alpha \tag{9}$$

where $\tau_{hps} = C_{uc}(R_{uc} + R_b)$, and α is determined by the initial state of U_c , U_L , i_L . Based on Equations (6)–(9), the iterative calculation process for passive hybrid power system can be accomplished with a discretization algorithm as described in Figure 4.

3. Simulation Experiments

For the passive hybrid power system, since the terminal voltages of battery pack and ultracapacitor pack are equal at any time, the current division between the battery pack and ultracapacitor pack is determined solely by their internal resistances and open-circuit voltages.

In order to show the different performance of a battery only power system and a hybrid power system, a comparison simulation experiment was carried out under the UDDS (Urban Dynamometer Driving Schedule). What’s more, in order to find the influence of different parameter matching on the performance of the passive hybrid power system, several simulation experiments were carried out comparing a fixed ultracapacitor pack and different battery packs with different cells. The basic parameters of the simulated hybrid electric vehicle are shown in Table 5.

Figure 4. Iterative algorithm for hybrid power system calculation.

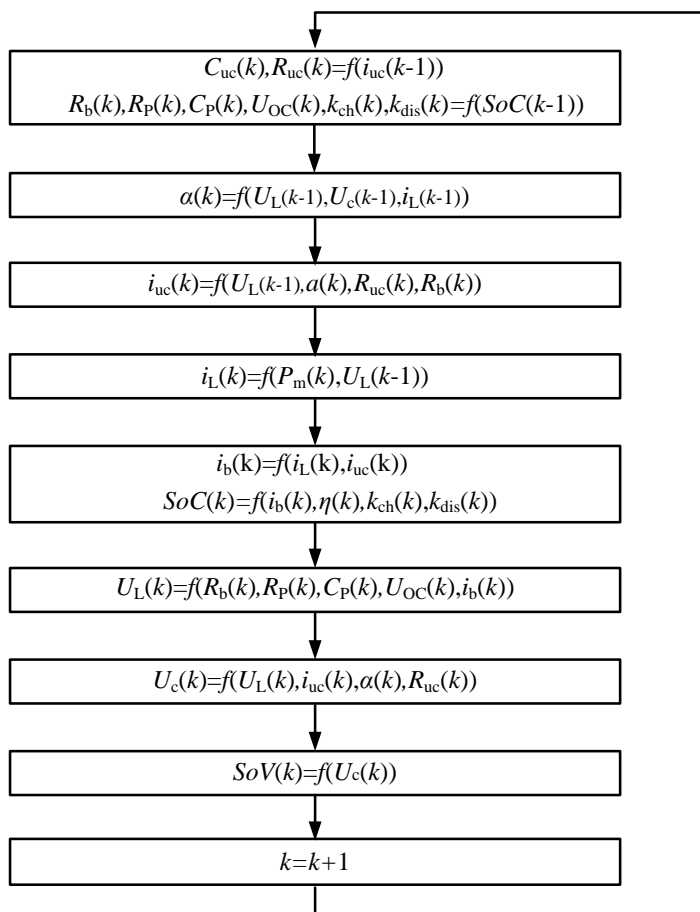


Table 5. The basic parameters of the simulated vehicle.

Vehicle	
Curb mass/kg	1320
Full load/kg	1845
Frontal area/m ²	2.53
Air resistance coefficient	0.36
Rolling radius/m	0.299
Hybrid Power System	
Battery type	lithium-ion battery
Nominal cell voltage/V	3.6
Nominal cell capacity/Ah	30
Number of cells/N _{bat}	88
Ultracapacitor	BMOD0500-16.2 V

Table 5. Cont.

Nominal module voltage/V	16
Nominal module capacity/F	500
Number of modules/ N_{uc}	21
Battery Only Power System	
Battery type	lithium-ion battery
Nominal cell voltage/V	3.6
Nominal cell capacity/Ah	30
Number of cells/ N_{bat}	88

Simulation results and comparisons between the batteries only power system and the hybrid power system are shown in Figures 5 and 6.

Figure 5. Comparison of current curves.

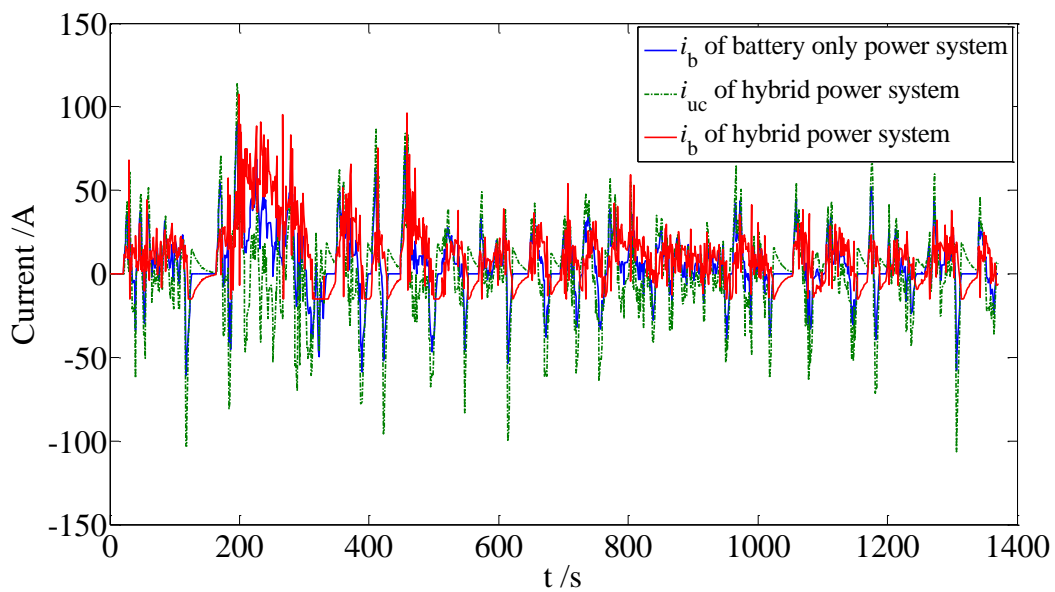
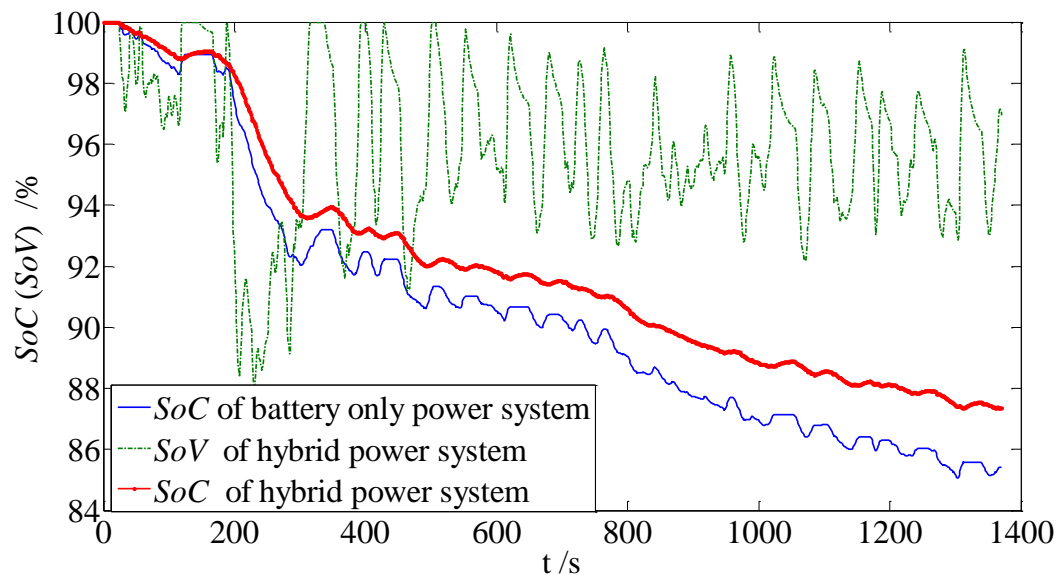


Figure 6. Comparison of SoC and SoV curves.



From Figure 5, the ultracapacitor pack absorbs the regenerative braking energy quickly and the impact of a big charging current on the battery pack is avoided. Furthermore, the charging current of the battery pack in the hybrid power system is less than 0.5 C, which would be very helpful to increase the cycle life of battery; while in power battery only power system, the charging current is nearly 2 C. However, inevitably, the battery pack charges the ultracapacitor pack for voltage balancing, so the discharging current of battery pack in the hybrid power system sees no significant reduction.

From Figure 6, because the ultracapacitor pack absorbs the braking energy actively and efficiently, and affords the additional peak power to meet the vehicle driving power requirement, the battery pack's output is smoothed, its *SoC* consumption is decreased by 2% and 7.78% electricity is saved after one UDSS, compared with the battery only drive system, which should be very helpful to extend the vehicle's driving range.

Figure 7 shows a comparison of the current histogram between the battery only power system and the hybrid power system. For the battery only power system, the duration of the charging current at 1 C is more than 100 s and at 2 C it is more than 30 s, while for the hybrid power system, the charging current of battery pack is less than 0.33 C, and the braking energy is absorbed by the ultracapacitor pack, which results in much higher efficiency, furthermore, the battery pack's working condition is greatly optimized.

Figure 7. Comparison of current histogram.

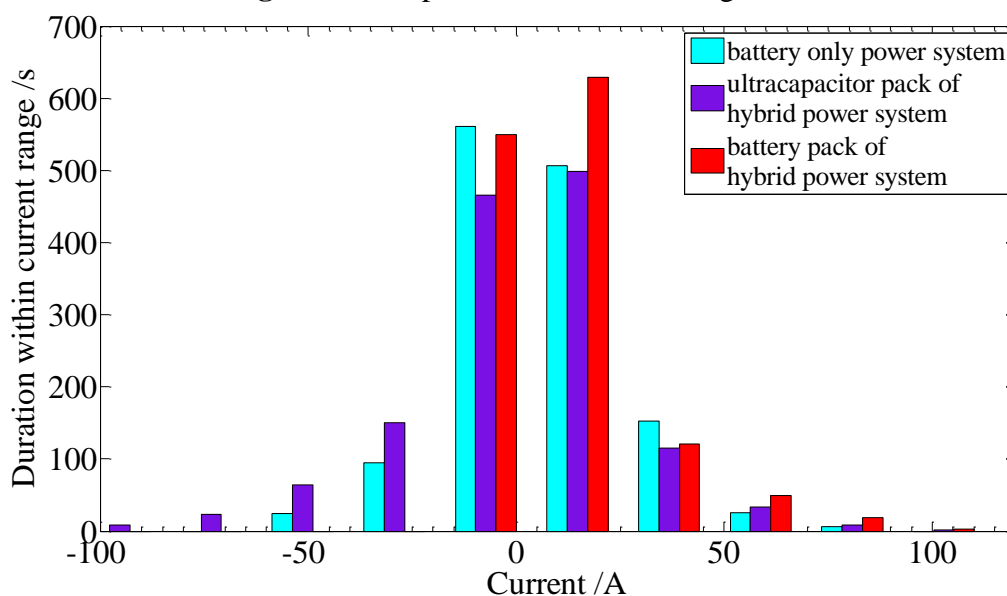


Table 6 lists the simulation results of difference of *SoC*, difference of *SoV* and *SoC* consumption savings and electricity savings percent compared with the battery only power system after one UDSS for different hybrid power systems. It was shown that some reasonable matching of battery pack and ultracapacitor pack parameters is necessary to achieve a higher performance. If the open-circuit voltage of the battery pack is lower than the maximum voltage of the ultracapacitor pack, the ultracapacitor pack would discharge a lot, which leads to low-*SoV* working of the ultracapacitor pack with a decrease of battery pack life. If the open-circuit voltage of the battery pack is larger than the maximum voltage of the ultracapacitor pack, the ultracapacitor pack's work is limited and the battery pack would discharge a lot, which makes it difficult to make the best of the advantages of the hybrid power system.

By comparison, when the maximum voltage of the ultracapacitor pack is designed to be equal to the open-circuit voltage of battery pack at $SoC = 90\%$, a maximum electricity saving is achieved.

Table 6. The list of simulation results of different hybrid power systems with different battery pack.

Battery Pack Number of Cells	Ultracapacitor Pack Number of Modules	$\Delta SoC/\%$	$\Delta SoV/\%$	SoC Consumption Saving/%	Electricity Saving/%
86	21	-13.7	-12.8	1.89	6.97
87	21	-13.2	-9.90	1.87	7.12
88	21	-12.5	-2.80	2.00	7.78
89	21	-13.9	-0.20	0.38	6.51
90	21	-14.1	-0.01	0.47	4.56

4. Conclusions

This paper establishes the dynamic model of a passive hybrid power system based on the Thevenin battery and ultracapacitor model. The simulation results show:

- (1) Combining high-energy-density batteries and high-power-density ultracapacitors for application in EVs can exploit the advantages of both of them and improve the performance of the power system;
- (2) For the hybrid power system, the impact of a big current on the battery pack is avoided. Its charging current is much lower than in the battery only power system, which will be very helpful to increase the cycle life of the battery for smooth working conditions;
- (3) Compared with a battery only power system, the SoC consumption of the battery pack in a hybrid power system is decreased by 2% and electricity savings of 7.78% are achieved;
- (4) Reasonable matching of the parameters of the passive hybrid power system is necessary to get a higher performance. It is verified that the maximum voltage of the ultracapacitor pack should be designed to be equal to the open-circuit voltage of battery pack at $SoC = 90\%$.

Acknowledgements

The financial support from the National High Technology Research and Development Program of China (No. 2008AA11A124) is gratefully acknowledged.

References

1. He, H.; Yan, S.; Xiao, Z. Integrated control method for a fuel cell hybrid system. *Asia-Pac. J. Chem. Eng.* **2009**, *4*, 68–72.
2. Kisacikoglu, M.; Uzunoglu, M.; Alam, M. Load sharing using fuzzy logic control in a fuel cell/ultracapacitor hybrid vehicle. *Int. J. Hydrogen Energy* **2009**, *34*, 1497–1507.
3. Nelson, R. Power requirements for batteries in hybrid electric vehicles. *J. Power Sources* **2000**, *91*, 2–26.

4. Xiong, R.; He, H.; Wang, Y.; Zhang, X. Study on ultracapacitor-battery hybrid power system for PHEV applications. *High Technol. Lett.* **2010**, *16*, 23–28.
5. Cheng, D.L.; Wismer, M.G. Active Control of Power Sharing in a Battery/Ultracapacitor Hybrid Source. In *Proceedings of 2nd IEEE Conference on Industrial Electronics and Applications*, Harbin, China, May 2007; pp. 2913–2918.
6. Henson, W. Optimal battery/ultracapacitor storage combination. *J. Power Sources* **2008**, *179*, 417–423.
7. Ozatay, E.; Zile, B.; Anstrom, J.; Brennan, S. Power distribution control coordinating ultracapacitors and batteries for electric vehicles. In *Proceedings of the 2004 American Control Conference*, Boston, MA, USA, June 2004; pp. 4716–4721.
8. Camara, M.; Gualous, H.; Gustin, F.; Berthon, A. Design and New Control of DC/DC Converters to Share Energy Between Supercapacitors and Batteries in Hybrid Vehicles. *IEEE Trans. Veh. Tech.* **2008**, *57*, 2721–2735.
9. Zhang, C.; Zhang, C.; Sharkh, S. Estimation of Real-Time Peak Power Capability of a Traction Battery Pack Used in an HEV. In *Proceedings of Asia-Pacific Power and Energy Engineering Conference (APPEEC)*, Chengdu, China, March 2010; pp. 1–6.
10. Idaho National Engineering & Environmental Laboratory. *Freedom CAR Battery Test Manual for Power-Assist Hybrid Electric Vehicles*; Assistant Secretary for Energy Efficiency and Renewable Energy (EE) Idaho Operations Office: Idaho Falls, ID, USA, 2003.
11. Elghaoui, L.; Lebret, H. Robust solutions to least-squares problems with uncertain data. *SIAM J. Matrix Anal. Appl.* **1997**, *18*, 1035–1064.
12. Nelms, R.M.; Cahela, D.R.; Tatarchuk, B.J. Modeling Double-Layer Capacitor Behavior Using Ladder Circuits. *IEEE Trans. Aero. Electron.* **2003**, *39*, 430–438.
13. Xiong, R.; He, H.; Zhang, X.; Wang, Y. Simulation study on hybrid ultracapacitor-battery power system for PHEV. In *Proceedings of IEEE The 2010 International Conference on Future Computer and Communication (ICFCC 2010)*, Wuhan, China, May 2010; pp. 496–500.